

## Supplemental Materials for

### **Spatiotemporal development of coexisting wave domains of Rho activity in cell cortex**

Siarhei Hladyszau<sup>1</sup>, Mary Kho<sup>1</sup>, Shuyi Nie<sup>1</sup>, Denis Tsygankov<sup>2\*</sup>

<sup>1</sup>School of Biology, Georgia Institute of Technology, Atlanta, GA.

<sup>2</sup>Wallace H. Coulter Department of Biomedical Engineering, Georgia Institute of Technology and Emory University, Atlanta, GA.

\*To whom correspondence should be addressed

Email: [denis.tsygankov@bme.gatech.edu](mailto:denis.tsygankov@bme.gatech.edu)

#### **This PDF file includes:**

Figures S1 to S3

#### **Other supplementary materials for this manuscript include:**

Videos S1 to S6.

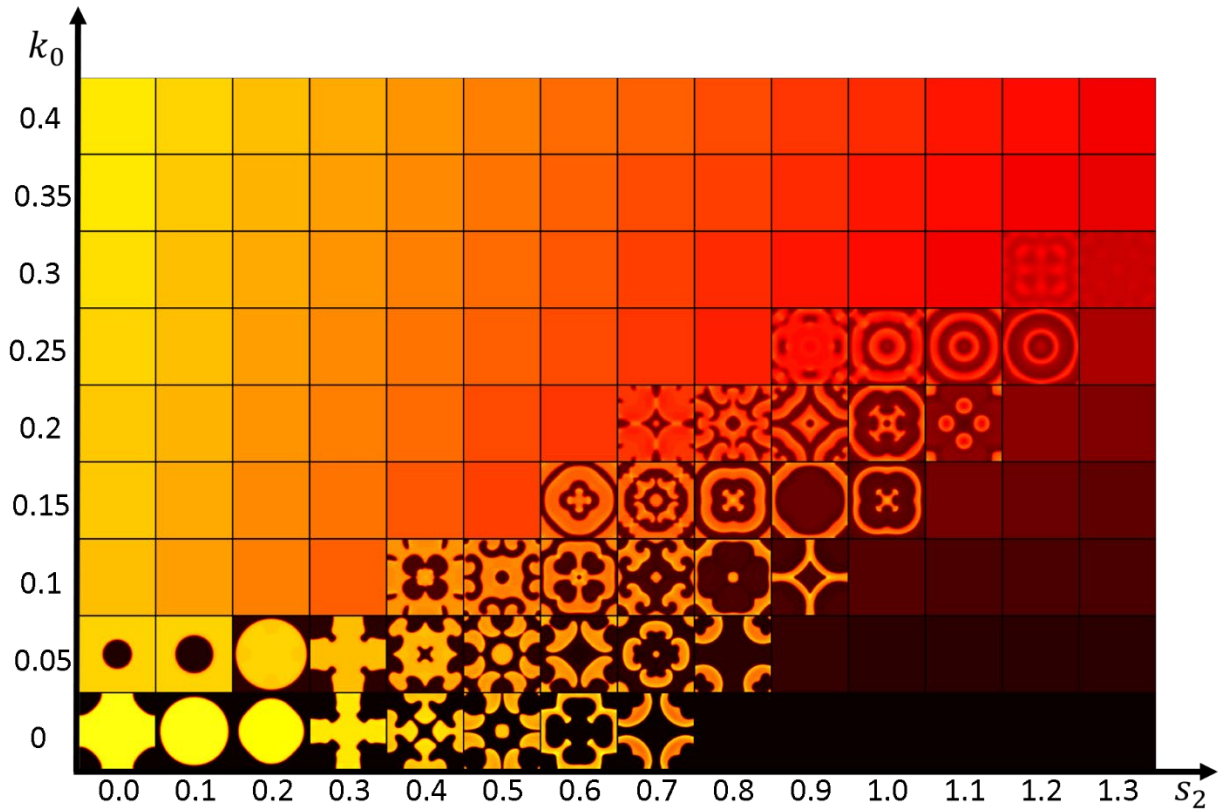


**Figure S1.** The result of our model simulations with nonhomogeneous initial conditions for a range of parameters  $k_0$  (the rate of basal activation) and  $s_2$  (the strength of negative feedback). The initial spike of excitation of component  $A$  in the middle of the simulation domain had the magnitude 5 au and the size  $10 \times 10$  grid steps ( $0.2 \times 0.2$  au). All simulations were performed on a square domain of size  $200 \times 200$  grid steps ( $4.0 \times 4.0$  au) with a time step 0.001 au and no-flux boundary conditions.

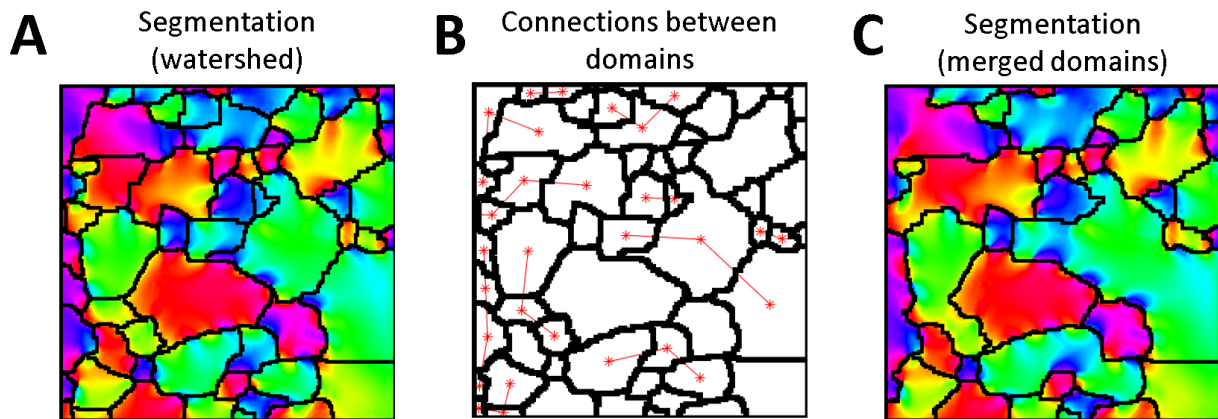


**Figure S2.** The workflow for the domains merging algorithm. **A.** Watershed segmentation used as an input for merging. **B.** A graphical representation of the connected domains as specified by the adjacency matrix  $A = (a_{ij})$  build based on the pairwise similarity of the domains. Here,  $a_{ij} = 1$  if the difference between the mean values of wave vector angles in domains  $i$  and  $j$  is less than 0.5 radians and if the length of the interface between the domains is larger than 10% of the square root of the area of the smallest of domains  $i$  and  $j$ . Otherwise,  $a_{ij} = 0$ . **C.** All the groups of connected domains are merged together by removing the interfaces between the adjacent domains while maintaining the 4-connectivity of the merged regions.

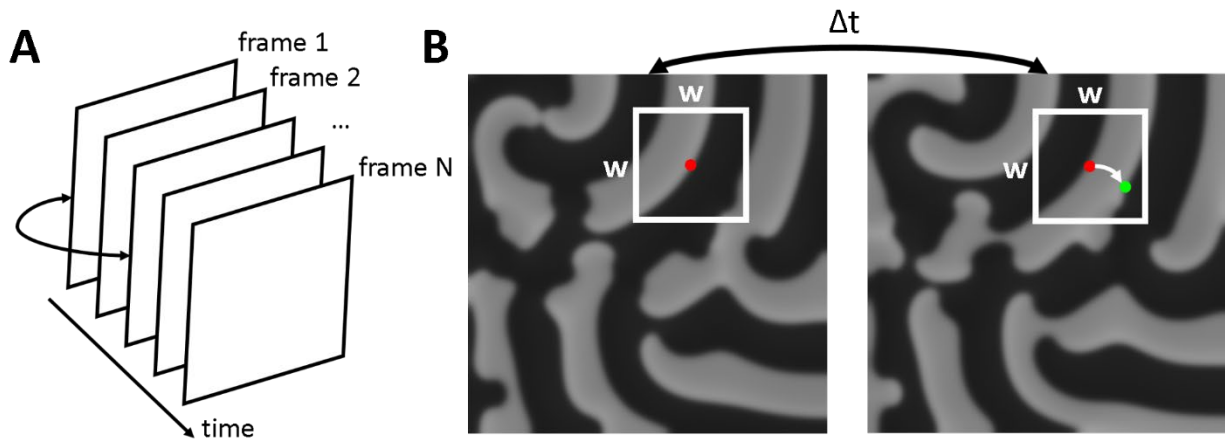


**Figure S3.** **A.** Temporal autocorrelation analysis for the time-series data. For the concentration of the activator  $A$ , we compute the correlation coefficients between each frame and the one that follows it after a time lag. To represent the dynamics of the pattern over time, we plotted the computed correlation coefficients as a function of time lag between frames. **B.** Algorithm for visualization of the wave-vector direction. For each node on the grid at the current state of the system (red dot) we find the node on the grid of the next time frame (green dot), which has the closest values of the concentration and the spatial gradient of the activator  $A$ . For that we apply the convolution operation with a weighted sum of all vectors starting from the red dot and ending in the pixels of the window of width  $w$  (white box). The weights depends on the difference in concentration values and the concentration gradient (see also the Methods section of the manuscript).